RSC Advances

PAPER

View Article Online
View Journal | View Issue

Cite this: *RSC Adv.*, 2023, **13**, 35659

Copper salt of a DABCO-based molten salt: a high-performance catalyst in the one-pot synthesis of 3,4-dihydropyrimidine and polyhydroquinoline derivatives†

Neamatullah Fekrat, Masoumeh Mazloumi and Farhad Shirini *

In this study, $[DABCO](SO_3H)_2CuCl_4$ as a novel DABCO-based molten salt with dual acidic functionality (Brønsted and Lewis) has been synthesized, characterized and used as a high-performance catalyst in the one-pot synthesis of 3,4-dihydropyrimidine and polyhydroquinoline derivatives. The identification of this catalyst was accomplished by using techniques such as infrared spectroscopy (FT-IR), X-ray diffraction (XRD), thermo gravimetric analysis (TGA), field emission scanning electron microscopy (FESEM) and energy dispersive X-ray (EDS) spectroscopy. Excellent efficiency, short reaction times, a simple working method and also use of a recyclable catalyst are the considerable advantages of this process.

Received 29th October 2023
Accepted 27th November 2023

DOI: 10.1039/d3ra07366a

rsc.li/rsc-advances

Introduction

One of the twelve principles of green chemistry is the usage of catalysts to design new synthetic processes.[1] Catalysts have been used for the purpose of environmental protection, economic benefits, and eliminating or reducing waste and destructive materials in the petrochemical industry, and chemical and pharmaceutical processes.[2] Among the various catalysts, ionic liquids have found a special place in green chemistry due to their unique properties as benign catalysts for the environment.[3] Nowadays, ionic liquids have ended up as a fervent topic of research in several fields of the experimental sciences, including chemistry, physics, biology, and engineering.[4] Ionic liquids are organic salts containing organic or inorganic cations and anions and their physical properties, polarity, and acidity/alkalinity can be adjusted by changing their cations and anions.[5,6] DABCO, as a result of having features such as having the nitrogen atom pair in the main structure, being consistent with the environment, being easy to carry, being non-toxic and having high reactivity has been used as a source of a suitable cation in the synthesis of various ionic liquids.[7,8] DABCO-based ionic liquids are not only used as catalysts in some organic transformations, but some of them can show biological activities such as antimicrobial and antibacterial ones.[9]

Metal-containing ionic liquids are a group of ionic liquids that combine the properties of ionic liquids with the magnetic, optical or catalytic properties of metal salts.[10] One of the most important features of these compounds is their controllable acidity, which makes them suitable for use as catalysts. Their acidic nature can be Lewis or Brønsted–Lewis type.[11] The performance of this type of ionic liquids as Lewis acids depends on the electrophilicity of the metal and the availability of its LUMO orbital.[12] Also, Brønsted–Lewis acidic ionic liquids (BLAILs) can be obtained from the reaction of Lewis acid metal salts or oxides with Brønsted acid ionic liquids. BLAILs are useful catalysts with dual acidic performance in many organic transformations, especially in multi-component reactions, because some synthesis processes require both types of acidity in one or more stages of the reaction. Common metals such as Al, Zn and Fe have been used as Lewis acids in Brønsted–Lewis acidic ionic liquids. Recently, Cu-containing ionic liquids such as $[(HSO_3)^3C_3C_1im][(1/2Cu^{2+})SO_4{}^{2-}]$ and $[(HSO_3)^3C_3C_1im]^-$ $[(1/2H^+ \cdot 1/4Cu^{2+})SO_4{}^{2-}]$ are prepared by changing the molar ratio of Cu to Brønsted acidic ionic liquids.[13]

Over the past few years, chemists have focused on the development of new methods that pose a lower risk to human health and environment, and based on this many synthetic processes have been modified. Among these, multi-component reactions have become more important than multi-step reactions due to their economic nature, energy and time-saving factor, and convergence in the field of organic synthesis. The synthesis of dihydropyrimidinones and polyhydroquinolines are interesting examples of such reactions.[14–17]

Dihydropyrimidinones and polyhydroquinolines are known because of their wide range of biological responses. Dihydropyrimidinones show anti-tumor,[18] anti-bacterial,[19] anti-viral,[20] anti-inflammatory,[21] calcium channel blocker,[22]

Department of Chemistry, College of Sciences, University of Guilan, Rasht 41335-19141, Iran. E-mail: shirini@guilan.ac.ir; Fax: +98 131 3233262; Tel: +981313233262

† Electronic supplementary information (ESI) available: FT-IR, ^{1}H NMR & ^{13}C NMR of new products. See DOI: https://doi.org/10.1039/d3ra07366a

antihypertensive,[23] and other activities. Also, important drug functions such as anti-tumor,[24] bronchodilators,[25] anti-atherosclerotic,[26] vasodilators, anti-inflammatory,[27] modulate calcium channels[28] and antidiabetic[29] properties have been reported for polyhydroquinoline derivatives.

These types of compounds are usually prepared *via* Bigenilli reaction (the one-pot three-component condensation of aldehydes, β-diketones and urea)[30–32] and Hantzsch condensation reaction (the one-pot four-component reaction of aldehydes, β-diketones, β-ketoesters and ammonium acetate), respectively.[33,34] Different strategies and reagents have been used in this field, which of them use of microwave, ultrasound, solid reagents with supports, oxides of transition metals,[35] Al_2O_3/$MeSO_3H$,[36] zirconia sulfuric acid,[37] metal oxide-MWCNTs nanocomposites[38] (in the synthesis of 3,4-dihydropyrimidinone), praseodymium(III) anchored on $CoFe_2O_4$MNPs,[39] $Yb(OTf)_3$,[40] nickel nanoparticle,[41] *p*-TSA,[42] zinc oxide,[43] Fe_3O_4@MCM-41@Cu-P2C,[44] and Cu(II)-PAA/M-MCM-41NC[45] (in the synthesis of polyhydroquinolines) are examples although these methods have undeniable advantages but most of them suffer from disadvantages such as the usage of expensive reagents, low efficiency, use of harmful heavy metal salts to the environment, tedious working methods, toxic solvents, being uneconomical, and problems in the preparation and non-recovery of catalysts. Therefore, the introduction of a high-performance catalytic system to synthesize these compounds and overcome all or some of the mentioned disadvantages is still required. In this article, $[DABCO](SO_3H)_2CuCl_4$ is introduced as a new acidic catalyst which is efficiently able to promote the synthesis of 3,4-dihydropyrimidinone and polyhydroquinoline derivatives under mild conditions with considerable yields in short times.

Experimental

All required chemicals and solvents were purchased from Fluka, Merck, and Aldrich chemical companies. All yields refer to their isolated products. The products were stabilized by comparison of their physical constants, IR, and NMR spectra with reported samples in the resources. Thin layer chromatography (TLC) was used on polygram SILG/UV 254 plates, for the determination of the purity of the substrates and monitoring of the progress of the reaction.

Preparation of $[DABCO](SO_3H)_2CuCl_4$

Diamino-bicyclo[2,2,2]octane (DABCO) (10 mmol, 1.12 g) was dissolved in 40 mL of the CH_2Cl_2. Then, $ClSO_3H$ (20 mmol, 1.330 mL) was added drop-wise in an ice bath (0 °C) to the prepared mixture during 5 min. The reaction was stirred for 2 hours at room temperature. After completion of the reaction, the obtained product was washed with diethyl ether and dried under vacuum. Finally, $[DABCO](SO_3H)_2Cl_2$ was achieved as a white compound.[46] In continue, $CuCl_2$ (10 mmol, 1.345 g) was added to $[DABCO](SO_3H)_2Cl_2$ (10 mmol, 3.45 g) in 40 mL of CH_3CN. Then, the reaction mixture was stirred for 24 h under reflux conditions and after completion of the reaction, the obtained compound was washed with diethyl ether and dried under vacuum. Finally, $[DABCO](SO_3H)_2CuCl_4$ was obtained as a green solid (4.79 g, 95% yield, Scheme 1).

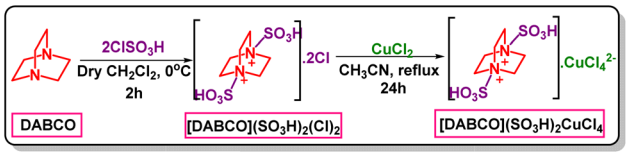

Scheme 1 Preparation of $[DABCO](SO_3H)_2CuCl_4$.

General procedure for the synthesis of 3,4-dihydropyrimidinone derivatives

20 mg of $[DABCO](SO_3H)_2CuCl_4$ was added to a mixture of aldehyde (1 mmol), ethyl acetoacetate (1 mmol) and urea (1.5 mmol) in a 10 mL round bottom flask and the reaction mixture was stirred in an oil bath at 120 °C in the absence of solvent. The reaction progress was controlled by thin layer chromatography (TLC) [*n*-hexane : ethyl acetate (2 : 6)]. At the end of the reaction, water (10 mL) was added to the reaction mixture and the product was separated from the catalyst by filtration. Finally, recrystallization from ethanol was performed in order to purify the requested product with high efficiency.

General procedure for the synthesis of polyhydroquinoline derivatives

In a 10 mL round bottom flask, 40 mg of $[DABCO](SO_3H)_2CuCl_4$ was added to a mixture of aldehyde (1 mmol), dimidone or 1,3-cyclohexanone (1 mmol), ammonium acetate (3 mmol), and ethyle or methyl acetoacetate (1 mmol). Then the reaction mixture was stirred under solvent-free conditions in an oil bath at 120 °C for an appropriate period of time. The progress of the reaction was followed by thin-layer chromatography (TLC) [*n*-hexane : ethyl acetate (2 : 6)]. After completion of the reaction, water (10 mL) was added to the reaction mixture and the product was separated from the catalyst by filtration. Finally, the product was purified by recrystallization from ethanol.

Results and discussion

Instrumentation

Melting points were measured by an electrothermal IA9100 melting point apparatus (United Kingdom) in capillary tubes. The Fourier-transform infrared spectros (FT-IR) were recorded with a VERTEX 70 (Brucker, Germany) instrument using KBr pellets for the obtained solid samples. X-ray diffraction (XRD) was performed on an X'Pert Pro instrument (Panalytical Company Netherlands). Field emission scanning electron microscopy (FESEM) was recorded using a TE-SCAN model Sigma VP (ZEISS Company in Germany). Thermogravimetric analysis (TGA) was performed on a TGA-DTA METTLER TGA/STTA 851 (Swiss).

Catalyst characterization

The FT-IR spectra of DABCO, $[DABCO](SO_3H)_2Cl_2$ and $[DABCO](SO_3H)_2CuCl_4$ are compared in Fig. 1. A large number

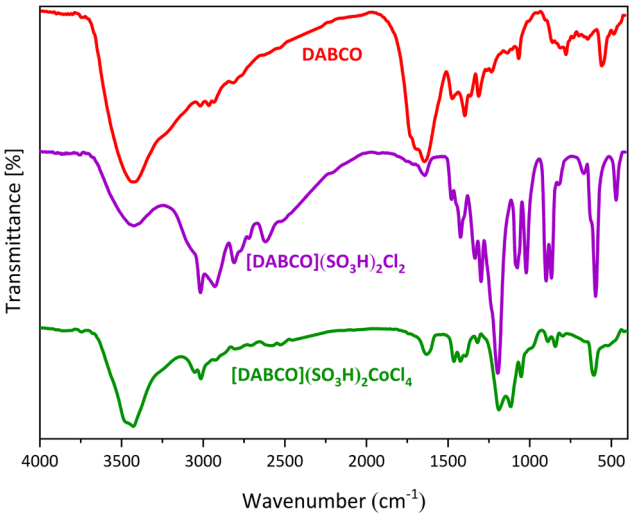

Fig. 1 FT-IR spectra of DABCO, $[DABCO](SO_3H)_2Cl_2$ and $[DABCO](SO_3H)_2CuCl_4$.

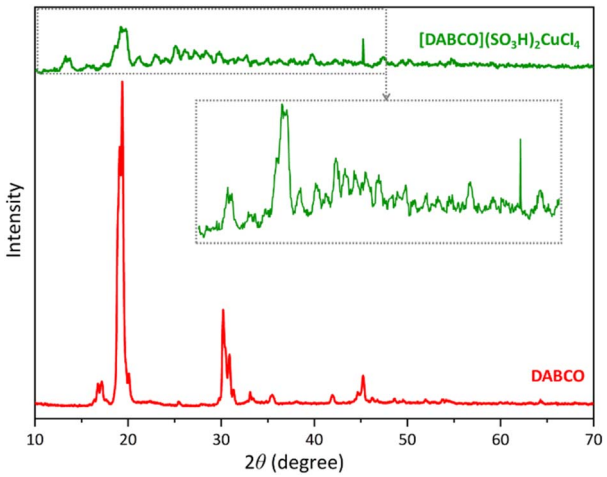

Fig. 3 XRD patterns of DABCO and $[DABCO](SO_3H)_2CuCl_4$.

of absorption bands are observed in DABCO's FT-IR spectrum which can be due to different types of stretching and bending vibrations in this compound. The appearance of new absorption bands in the FT-IR spectrum of $[DABCO](SO_3H)_2Cl_2$ in the regions of 1179 cm^{-1} and 581 cm^{-1} can be attributed to the vibrations related to S=O and S–O, respectively.[47] In addition, the absorption bands at 1852 cm^{-1} and 885 cm^{-1} are related to N–S bond vibrations.[48] A number of absorption bands in the FT-IR spectrum of $[DABCO](SO_3H)_2CuCl_4$ catalyst have been removed or reduced in intensity, which can be due to the presence of copper metal and the created limitations in the vibrations of the rings.

The thermogravimetric analysis (TGA) was performed in order to compare the thermal stability of DABCO and $[DABCO](SO_3H)_2CuCl_4$ (Fig. 2). As can be seen, DABCO completely degrades before 150 °C, while $[DABCO](SO_3H)_2CuCl_4$ catalyst has higher thermal stability that can be due to hydrogen bonding and the presence of copper metal in the structure of the catalyst. In the TGA curve of the $[DABCO](SO_3H)_2CuCl_4$, two weight losses are observed in the range of 150–250 °C and 250–450 °C, which can be the result of the thermal degradation of DABCO and sulfonic groups in its structure.

The X-ray diffraction patterns of DABCO and $[DABCO](SO_3H)_2CuCl_4$ are shown in Fig. 3. In the diffraction pattern related to DABCO, ten peaks appeared around 2θ = 16.7, 17.2, 18.5, 19.4, 30.2, 30.9, 33.15, 35.46, 41.96 and 45.24 confirming DABCO.[49] The intensity of these peaks has decreased in the diffraction pattern of the catalyst, which is due to decreasing its crystallinity. Furthermore, the increase in the number of peaks in this pattern can be a result of the presence of $CuCl_4$ in the catalyst structure.

The results of EDS analysis obtained from $[DABCO](SO_3H)_2CuCl_4$ indicate the presence of all expected elements (C,

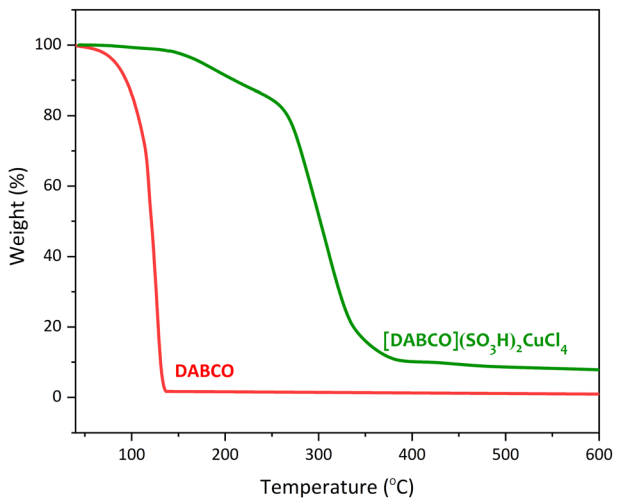

Fig. 2 TGA curves of DABCO and $[DABCO](SO_3H)_2CuCl_4$.

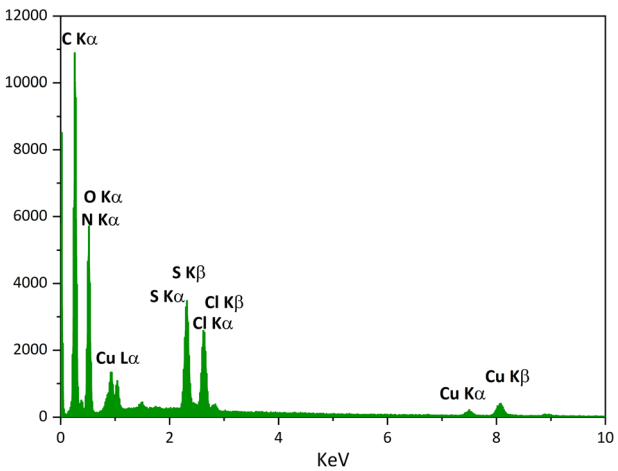

Fig. 4 EDS analysis of $[DABCO](SO_3H)_2CuCl_4$.

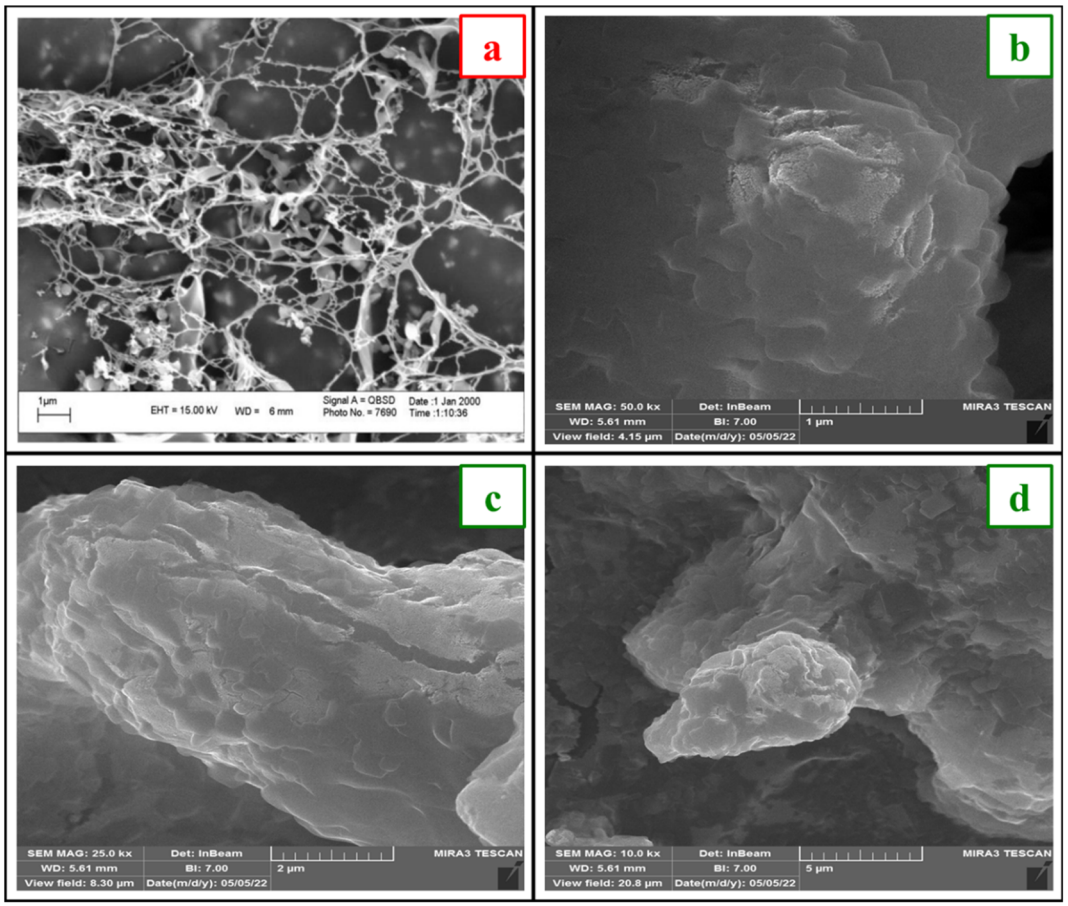

Fig. 5 FESEM images of DABCO (a (1 μm)) and $[DABCO](SO_3H)_2CuCl_4$ (b (1 μm), c (2 μm), d (5 μm)).

Table 1 Optimization of the reaction conditions for the synthesis of 3,4-dihydropyrimidinones catalyzed by $[DABCO](SO_3H)_2CuCl_4$

Entry	Catalyst (mg)	Temperature (°C)	Solvent	Time (min)	Conversion (%)
1	20	80 °C	Solvent free	25	Mixed products
2	20	100 °C	Solvent free	15	100
3	30	100 °C	Solvent free	14	100
4	40	100 °C	Solvent free	10	100
5	20	120 °C	Solvent free	10	100
6	30	120 °C	Solvent free	9	100
7	40	120 °C	Solvent free	8	100
8	20	Reflux	H_2O	70	Not completed
9	20	Reflux	C_2H_5OH	75	Not completed
10	20	80 °C	$C_2H_5OH : H_2O$ (1 : 1)	80	Not completed

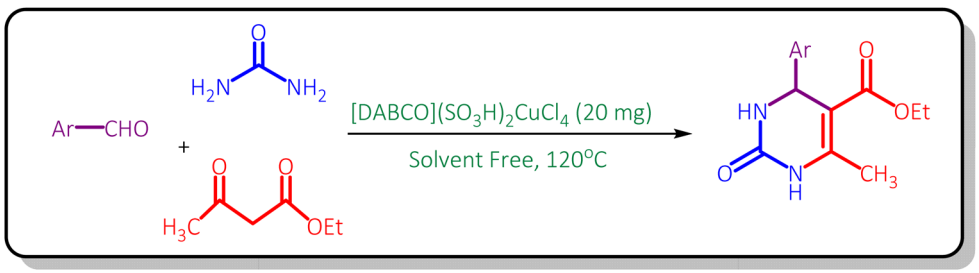

Scheme 2 Synthesis of 3,4-dihydropyrimidinone derivatives catalyzed by $[DABCO](SO_3H)_2CuCl_4$.

Table 2 Synthesis of 3,4-dihydropyrimidinone derivatives in the presence of $[DABCO](SO_3H)_2CuCl_4$[a]

Entry	Aldehyde	Product	Time (min)	Yield[a] (%)	Melting point (°C) Found	Reported
1	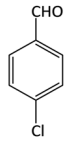	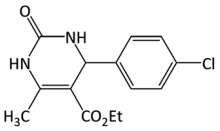	10	92	195–197	198–202 (ref. 50)
2	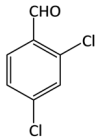	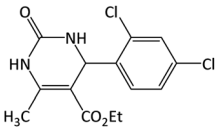	25	94	231–233	228–230 (ref. 51)
3	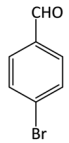	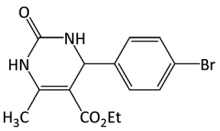	30	94	228–230	232–234 (ref. 52)
4	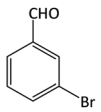	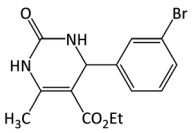	28	93	197–199	185–187 (ref. 53)
5	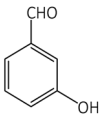	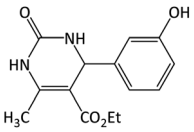	9	95	159–160	165–167 (ref. 54)
6	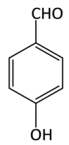	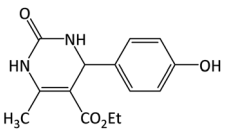	15	92	194–196	197–199 (ref. 55)
7	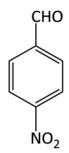	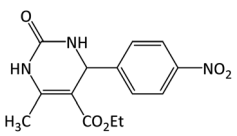	14	95	204–206	205–207 (ref. 56)
8	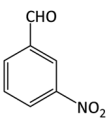	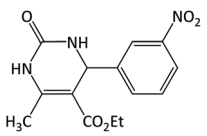	10	93	217–218	224–226 (ref. 57)
9	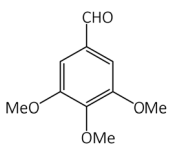	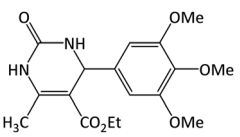	9	97	213–215	213–215 (ref. 58)
10	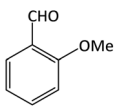	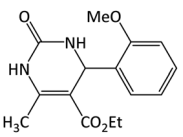	22	96	245–247	252–254 (ref. 59)

Table 2 (*Contd.*)

Entry	Aldehyde	Product	Time (min)	Yield[a] (%)	Melting point (°C) Found	Reported
11	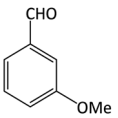	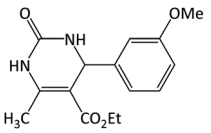	14	95	210–212	207–209 (ref. 60)
12	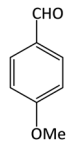	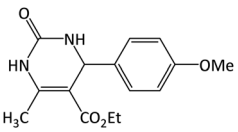	45	80	200–202	205–207 (ref. 61)
13	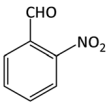	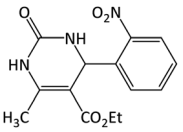	16	98	235–237	233–235 (ref. 62)
14	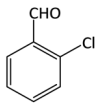	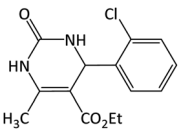	30	94	220–222	219–221 (ref. 61)
15	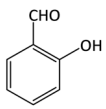	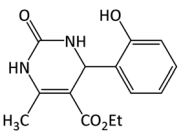	22	90	190–192	200–202 (ref. 63)
16	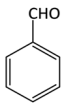	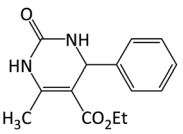	32	88	195–197	201–203 (ref. 64)
17	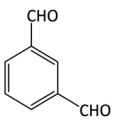	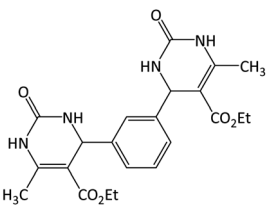	8	94	211–213	212–214 (ref. 65)

[a] Isolated yields.

O, N, S, Cl, Cu) in the structure of the sample (Fig. 4) showing its successful formation.

Fig. 5 shows the field emission scanning electron microscopy (FESEM) images of DABCO and [DABCO](SO$_3$H)$_2$CuCl$_4$ which specifies the surface morphology, size distribution and particle shape of them. The pictures show that DABCO has a string structure with tiny holes. While the catalyst has continuous particles and a rough surface which can be due to the presence of intermolecular hydrogen bonds between and also dipole–dipole interaction between the catalyst particles.

Catalytic activity

After successful identification of the prepared catalyst, it has been suggested that this reagent may be able to accelerate reactions that require an acidic catalyst. Therefore, we decided to study the performance of this catalyst in the synthesis of 3,4-dihydropyrimidinone derivatives. In this regard, the condensation of 4-chlorobenzaldehyde, ethyl acetate, and urea is selected as the model reaction and the effect of the amounts of the catalyst, solvent, and temperature was investigated on it (Table 1).

Table 3 Optimization of the reaction conditions for the synthesis of polyhydroquinoline catalyzed by $[DABCO](SO_3H)_2CuCl_4$

Entry	Catalyst (mg)	Temperature (°C)	Solvent	Time (min)	Conversion (%)
1	10	100 °C	Solvent free	20	Not completed
2	20	100 °C	Solvent free	11	100
3	30	100 °C	Solvent free	10	100
4	40	100 °C	Solvent free	10	100
5	10	120 °C	Solvent free	15	Not completed
6	20	120 °C	Solvent free	10	100
7	30	120 °C	Solvent free	9	100
8	40	120 °C	Solvent free	6	100
9	40	Reflux	C_2H_5OH	58	Not completed
10	40	Reflux	H_2O	65	Not completed
11	40	80 °C	$C_2H_5OH : H_2O$ (1 : 1)	70	Not completed

It was found that the reaction can be performed in the absence of solvent. It should be mentioned that the reaction in solvents such as water and ethanol even under reflex conditions did not proceed considerably. Further investigations on the influence of the amounts of the catalyst and temperature clarified that 20 mg of the catalyst at 120 is enough to accomplish the reaction in shortest time with good efficiency (Table 1, entry 5) (Scheme 2).

After determining optimal conditions, in order to generalize this method, a variety of aromatic aldehydes containing electron-donating or electron-withdrawing functional groups in *ortho*, *meta*, and *para* positions of the aromatic ring were used to synthesize a variety of 3,4-dihydropyrimidinone derivatives under these conditions. The results show that all derivatives are synthesized in short reaction time with high yields (Table 2).

After the successful application of $[DABCO](SO_3H)_2CuCl_4$ as a catalyst in the synthesis of 3,4-dihydropyrimidinones, we decided to study the ability and efficiency of this reagent in the synthesis of polyhydroquinoline derivatives *via* Hantzsch condensation. In the first step, to find the optimum conditions, a model reaction was performed with a mixture of 4-hydroxybenzaldehyde, ethyl acetoacetate, dimedone, and ammonium acetate in the presence of different amounts of the catalyst in the presence and absence of solvent at a variety of temperatures (Table 3).

The results obtained show that the reaction of aldehyde (1 mmol) with ethyl acetoacetate (1 mmol), dimedon (1 mmol) and ammonium acetate (2 mmol) was performed in the presence of 40 mg of the catalyst at 120 °C under solvent-free conditions in less times with higher yields (Table 3, entry 8) (Scheme 3).

In continue and in order to generalize the optimized reaction conditions, a wide range of aldehydes and different β-diketones were used in this four-component condensation. It was found that this method is very efficient for the conversion of aromatic aldehydes containing electron-donor and electron-acceptor substituents, to their corresponding polyhydroquinoline derivatives with good yields in short times (Table 4).

A suggested mechanism for the studied reactions in the presence of $[DABCO](SO_3H)_2CuCl_4$ as the catalyst is shown in Scheme 4. Path (a) is related to the synthesis of 3,4-dihydropyrimidinones. At the first step of this path, the carbonyl group of the aldehyde is activated by the acidic catalyst producing the intermediate (**I**) through nucleophilic attak of urea. Then, the reaction of the intermediate (**I**) and the activated ethyl acetate by the catalyst produces the intermediate (**II**). Finally, intermolecular cyclization of this intermediate and removal of a molecule of water provides the desired product. Path (b) shows the mechanism of the synthesis of polyhydroquinoline derivatives. Firstly, aldehyde and β-diketone (dimedone or 1,3-cyclohexanedione) be converted to their active form by the catalyst and then the Knoevenagel condensation of them lead to the intermediate **I′**. On the other hand, activated β-ketoester (ethyl

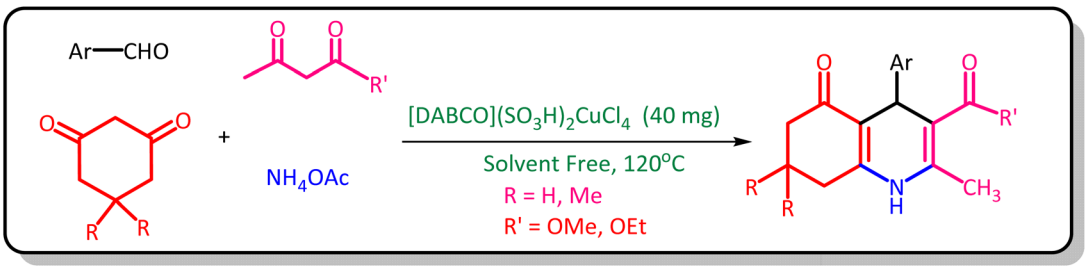

Scheme 3 Synthesis of polyhydroquinoline derivatives catalyzed by $[DABCO](SO_3H)_2CuCl_4$.

Table 4 Synthesis of polyhydroquinolines derivatives in the presence of $[DABCO](SO_3H)_2CuCl_4$[a]

Entry	Aldehyde	R	R'	Time (min)	Yield[a] (%)	Melting point (°C) Found	Melting point (°C) Literature
1	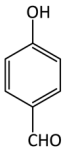	CH_3	OEt	6	98	230–232	232–234 (ref. 29)
2	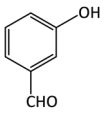	CH_3	OEt	10	93	214–216	217–219 (ref. 66)
3	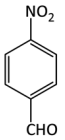	CH_3	OEt	27	90	222–224	228–232 (ref. 9)
4	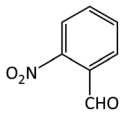	CH_3	OEt	21	93	191–193	198–200 (ref. 67)
5	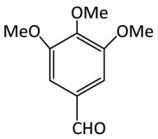	CH_3	OEt	11	93	204–206	199–200 (ref. 68)
6	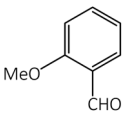	CH_3	OEt	15	96	244–246	248–250 (ref. 49)
7	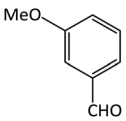	CH_3	OEt	18	90	195–197	198–200 (ref. 49)
8	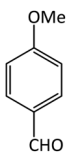	CH_3	OEt	35	90	240–242	246–248 (ref. 69)
9	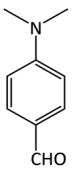	CH_3	OEt	8	90	226–228	231–233 (ref. 49)
10	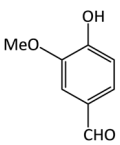	CH_3	OEt	6	98	215–217	211–213 (ref. 29)
11	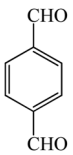	CH_3	OEt	8	88	309–311	305–307 (ref. 49)

Table 4 (*Contd.*)

Entry	Aldehyde	R	R'	Time (min)	Yield[a] (%)	Melting point (°C) Found	Melting point (°C) Literature
12	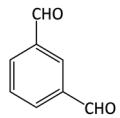	CH_3	OEt	10	88	288–290	281–282 (ref. 49)
13	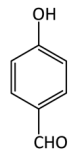	H	OEt	2	98	245–247	244–246 (ref. 49)
14	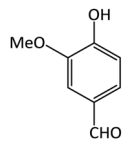	H	OEt	2	92	223–225	228–230 (ref. 9)
15	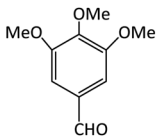	H	OEt	11	94	160–162	157–160 (ref. 70)
16	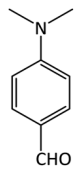	H	OEt	3	92	211–213	204–206 (ref. 49)
17	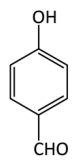	CH_3	OMe	8	85	240–242	232–234 (ref. 71)
18	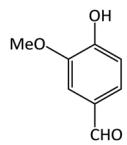	CH_3	OMe	4	94	256–258	252–256 (ref. 67)
19	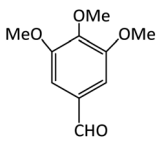	CH_3	OMe	10	90	258–260	260–262 (ref. 72)
20	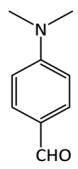	CH_3	OMe	8	90	252–254	258–259 (ref. 49)

[a] Isolated yields.

acetoacetate and methyl acetoacetate) reacted with the ammonia obtained from ammonium acetate and converted to enamine (intermediate **II′**) by removing a molecule of water. Then, enamine reacts with intermediate (**I′**) *via* Michael addition. Finally, poly-hydroquinoline derivatives are produced by nucleophilic attack of nitrogen on the

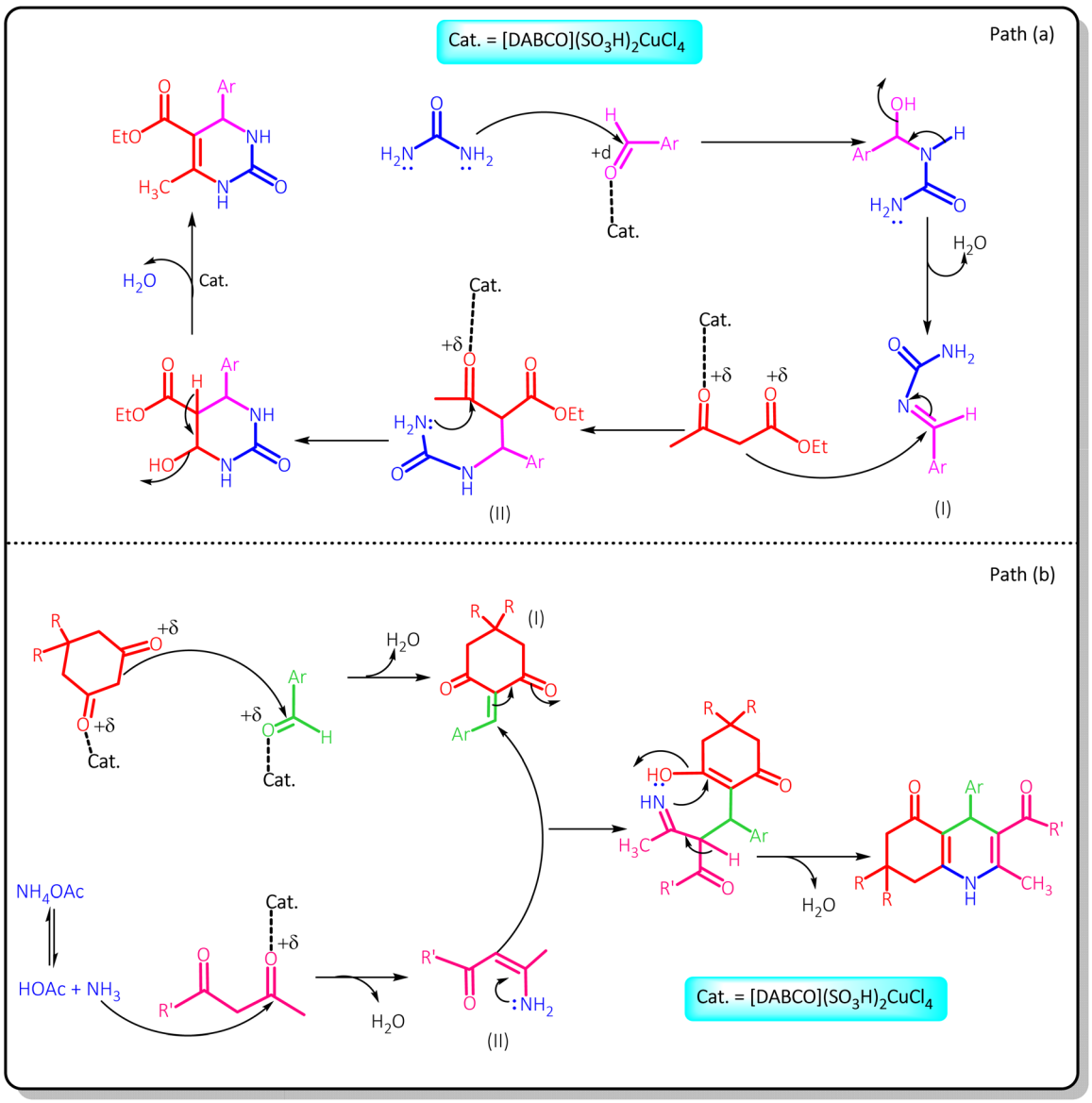

Scheme 4 The proposed mechanism for the synthesis 3,4-dihydropyrimidinones and polyhydroquinolines in the presence of $[DABCO](SO_3H)_2CuCl_4$.

carbonyl group, intermolecular cyclization and removal of a water molecule.

Table 5 compares the performance of $[DABCO](SO_3H)_2CuCl_4$ in the synthesis of one of the 3,4-dihydropyrimidine and polyhydroquinoline derivatives with some of the previous reported catalysts. The results of this comparison clearly show the superiority of this catalyst in the reduction of the amounts of the catalyst, and reaction times, and increasement of the yields over the other catalytic systems reported in the sources.

To evaluate the recyclability of the catalyst, the reaction of 4-hydroxybenzaldehyde with daimedone, ethyl acetoacetate, and ammonium acetate under optimized reaction conditions was investigated. After the completion of the reaction, water was added and the catalyst was separated from the product by filtration. After drying, the recycled catalyst was reused for the same reaction. This process was repeated six times. In all reactions, there was no significant change in the time and yield of the products, which clearly demonstrates the practical recyclability of this catalyst (Fig. 6). Comparison of the FT-IR of the recycled and freshly prepared catalyst shows it stability during the course of the reaction.

Table 5 Comparison of the results obtained from the synthesis of ethyl 4-(4-chlorophenyl)-6-methyl-2-oxo-1,2,3,4-tetrahydropyrimidine-5-carboxylate and ethyl 4-(4-hydroxyphenyl)-2,7,7-trimethyl-5-oxo-1,4,5,6,7,8-hexahydroquinoline-3-carboxylate in the presence of $[DABCO](SO_3H)_2CuCl_4$ with some of the best results reported in the references

Entry	Catalyst (mg) [ref.]	Reaction conditions	Time (min)	Yield (%)	Product
1	Fe_3O_4@SiO_2/TES Mo^+HSO_4 (60)[73]	C_2H_5OH/78 °C	60	87	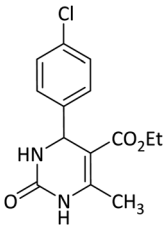
2	Nafion-Ga (200)[74]	Solvent free/110 °C	60	94	
3	$NH_4H_2PO_4$/MCM-41 (40)[75]	Solvent free/100 °C	219	72	
4	Al_2O_3–SO_3H (31)[76]	Solvent free/120 °C	96	94	
5	$Al(HSO_4)_3$ (27)[76]	Solvent free/100 °C	55	90	
6	Phytic acid (66)[77]	Solvent free/100 °C	180	88	
7	$[DABCO](SO_3H)_2CuCl_4$ (20) [this work]	Solvent free/120 °C	6	96	
8	$[TBA]_2[W_6O_{19}]$ (132)[78]	Solvent free/110 °C	20	91	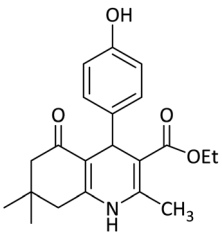
9	CAN (55)[79]	C_2H_5OH/reflux	120	89	
10	$[(DABCO)_2C_3H_5OH]\cdot 2Cl$ (30)[9]	Solvent free/120 °C	15	90	
11	Aluminized polyborate (75)[80]	Solvent free/100 °C	25	89	
12	Cell-Pr-$NHSO_3H$ (50)[81]	C_2H_5OH/reflux	50	85	
13	MCM-41@Serine@Cu(II) (50)[82]	C_2H_5OH/reflux	130	91	
14	VDDAP (100)[83]	C_2H_5OH : H_2O/r.t	90	73	
15	$[DABCO](SO_3H)_2CuCl_4$ (40) [this work]	Solvent free/120 °C	6	96	

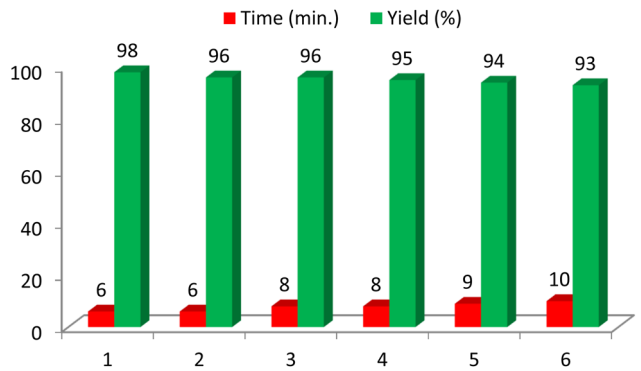

Fig. 6 Reusability of the $[DABCO](SO_3H)_2CuCl_4$.

Conclusions

In conclusion, in this study, the preparation of $[DABCO](SO_3H)_2CuCl_4$ was described in detail. After identification, it was used as an adequate and cost-effective catalyst in the synthesis of 3,4-dihydropyrimidinone and polyhydroquinoline derivatives. This method shows advantages such as high reaction rates, high efficiency, no use of hazardous organic solvents, ease of the catalyst preparation, and use of a reusable catalyst.

Conflicts of interest

There are no conflicts to declare.

Acknowledgements

We are thankful to the Research Council of the University of Guilan for the partial support of this work.

References

1 K. J. Ardila-Fierro and J. G. Hernández, *ChemSusChem*, 2021, **14**, 2145–2162.
2 P. Sarma, A. K. Dutta and R. Borah, *Catal. Surv. Asia*, 2017, **21**, 70–93.
3 C. Dai, J. Zhang, C. Huang and Z. Lei, *Chem. Rev.*, 2017, **117**, 6929–6983.
4 B. Wang, L. Qin, T. Mu, Z. Xue and G. Gao, *Chem. Rev.*, 2017, **117**, 7113–7131.
5 C. G. Yoo, Y. Pu and A. J. Ragauskas, *Curr. Opin. Green Sustainable Chem.*, 2017, **5**, 5–11.
6 C. Verma, E. E. Ebenso and M. Quraishi, *J. Mol. Liq.*, 2019, **276**, 826–849.
7 N. Jamasbi, M. Irankhah-Khanghah, F. Shirini, H. Tajik and M. S. N. Langarudi, *New J. Chem.*, 2018, **42**, 9016–9027.
8 R. Gupta, M. Yadav, R. Gaur, G. Arora, P. Rana, P. Yadav, A. Adholeya and R. K. Sharma, *ACS Omega*, 2019, **4**, 21529–21539.
9 M. Zabihzadeh, A. Omidi, F. Shirini, H. Tajik and M. S. N. Langarudi, *J. Mol. Struct.*, 2020, **1206**, 127730–127740.
10 C. Chiappe, C. S. Pomelli, U. Bardi and S. Caporali, *Phys. Chem. Chem. Phys.*, 2012, **14**, 5045–5051.
11 K. Li, H. Choudhary and R. D. Rogers, *Curr. Opin. Green Sustainable Chem.*, 2018, **11**, 15–21.
12 J. Estager, J. Holbrey and M. Swadźba-Kwaśny, *Chem. Soc. Rev.*, 2014, **43**, 847–886.
13 A. S. Amarasekara, *Chem. Rev.*, 2016, **116**, 6133–6183.
14 M.-N. Chen, L.-P. Mo, Z.-S. Cui and Z.-H. Zhang, *Curr. Opin. Green Sustainable Chem.*, 2019, **15**, 27–37.
15 R. Afshari and A. Shaabani, *ACS Comb. Sci.*, 2018, **20**, 499–528.

16 Z. Zhang, Y. You and C. Hong, *Macromol. Rapid Commun.*, 2018, **39**, 1800362–1800374.
17 C. Lamberth, *Bioorg. Med. Chem.*, 2020, **28**, 115471–115483.
18 R. V. Patil, J. U. Chavan, D. S. Dalal, V. S. Shinde and A. G. Beldar, *ACS Comb. Sci.*, 2019, **21**, 105–148.
19 M. Khodamorady, S. Sohrabnezhad and K. Bahrami, *Polyhedron*, 2020, **178**, 114340–114353.
20 N. Khaldi-Khellafi, M. Makhloufi-Chebli, D. Oukacha-Hikem, S. T. Bouaziz, K. O. Lamara, T. Idir, A. Benazzouz-Touami and F. Dumas, *J. Mol. Struct.*, 2019, **1181**, 261–269.
21 E. Vessally, A. Hassanpour, R. Hosseinzadeh-Khanmiri, M. Babazadeh and J. Abolhasani, *Monatsh. Chem.*, 2017, **148**, 321–326.
22 Y. Liu, Y. Dang, D. Yin, X. Yang, L. Yang and Q. Zou, *Res. Chem. Intermed.*, 2020, **46**, 547–555.
23 A. R. Kiasat and J. Davarpanah, *Res. Chem. Intermed.*, 2015, **41**, 2991–3001.
24 M. Hajjami and B. Tahmasbi, *RSC Adv.*, 2015, **5**, 59194–59203.
25 A. Ghorbani-Choghamarani, B. Tahmasbi, P. Moradi and N. Havasi, *Appl. Organomet. Chem.*, 2016, **30**, 619–625.
26 A. Ghorbani-Choghamarani, M. Mohammadi, T. Tamoradi and M. Ghadermazi, *Polyhedron*, 2019, **158**, 25–35.
27 J. Davarpanah, M. Ghahremani and O. Najafi, *J. Mol. Struct.*, 2019, **1177**, 525–535.
28 A. Maleki, F. Hassanzadeh-Afruzi, Z. Varzi and M. S. Esmaeili, *Mater. Sci. Eng. C*, 2020, **109**, 110502–110536.
29 R. R. Harale, P. V. Shitre, B. R. Sathe and M. S. Shingare, *Res. Chem. Intermed.*, 2017, **43**, 3237–3249.
30 K. Selvakumar, T. Shanmugaprabha, M. Kumaresan and P. Sami, *Synth. Commun.*, 2018, **48**, 223–232.
31 L. Moradi and M. Tadayon, *J. Saudi Chem. Soc.*, 2018, **22**, 66–75.
32 K. A. Dilmaghani, B. Zeynizadeh and H. Parasajam, *Phosphorus, Phosphorus, Sulfur Relat. Elem.*, 2012, **187**, 544–553.
33 S. Mondal, B. C. Patra and A. Bhaumik, *ChemCatChem*, 2017, **9**, 1469–1475.
34 S. K. Das, S. Mondal, S. Chatterjee and A. Bhaumik, *ChemCatChem*, 2018, **10**, 2488–2495.
35 P. Gogoi, A. K. Dutta and R. Borah, *Catal. Lett.*, 2017, **147**, 674–685.
36 H. Sharghi and M. Jokar, *Synth. Commun.*, 2009, **39**, 958–979.
37 M. M. Hosseini, E. Kolvari, N. Koukabi, M. Ziyaei and M. A. Zolfigol, *Catal. Lett.*, 2016, **146**, 1040–1049.
38 J. Safari and S. Gandomi-Ravandi, *J. Mol. Struct.*, 2014, **1074**, 71–78.
39 T. Tamoradi, S. M. Mousavi and M. Mohammadi, *New J. Chem.*, 2020, **44**, 3012–3020.
40 L.-M. Wang, J. Sheng, L. Zhang, J.-W. Han, Z.-Y. Fan, H. Tian and C.-T. Qian, *Tetrahedron*, 2005, **61**, 1539–1543.
41 S. B. Sapkal, K. F. Shelke, B. B. Shingate and M. S. Shingare, *Tetrahedron Lett.*, 2009, **50**, 1754–1756.
42 S. R. Cherkupally and R. Mekala, *Chem. Pharm. Bull.*, 2008, **56**, 1002–1004.
43 F. M. Moghaddam, H. Saeidian, Z. Mirjafary and A. Sadeghi, *J. Iran. Chem. Soc.*, 2009, **6**, 317–324.
44 M. Nikoorazm and Z. Erfani, *Chem. Phys. Lett.*, 2019, **737**, 136784–136794.
45 S. Vaysipour, Z. Rafiee and M. Nasr-Esfahani, *Polyhedron*, 2020, **176**, 114294–114333.
46 N. Seyyedi, F. Shirini and M. S. N. Langarudi, *RSC Adv.*, 2016, **6**, 44630–44640.
47 M. Abedini, F. Shirini, J. Mohammad-Alinejad Omran, M. Seddighi and O. Goli-Jolodar, *J. Iran. Chem. Soc.*, 2016, **42**, 4443–4458.
48 O. Goli-Jolodar, F. Shirini and M. Seddighi, *J. Nanosci. Nanotechnol.*, 2018, **18**, 591–603.
49 O. Goli-Jolodar, F. Shirini and M. Seddighi, *RSC Adv.*, 2016, **6**, 26026–26037.
50 D. Azarifar, Y. Abbasi and O. Badalkhani, *J. Iran. Chem. Soc.*, 2016, **13**, 2029–2038.
51 S. Rezayati, F. Kalantari, A. Ramazani, S. Sajjadifar, H. Aghahosseini and A. Rezaei, *Inorg. Chem.*, 2021, **61**, 992–1010.
52 Y. T. Wang, G. M. Tang and Y. S. Wu, *Appl. Organomet. Chem.*, 2020, **34**, 1–19.
53 S. Kargar, D. Elhamifar and A. Zarnegaryan, *J. Phys. Chem. Solids*, 2020, **146**, 109601–109640.
54 Z. Ghadamyari, A. Shiri, A. Khojastehnezhad and S. M. Seyedi, *Appl. Organomet. Chem.*, 2019, **33**, 1–10.
55 K. A. Dilmaghani, B. Zeynizadeh and M. Amirpoor, *Phosphorus Sulfur Silicon Relat. Elem.*, 2013, **188**, 1634–1642.
56 Z.-B. Xie, L.-H. Fu, J. Meng, J. Lan, Z.-Y. Hu and Z.-G. Le, *Bioorg. Chem.*, 2020, **101**, 103949–103956.
57 R. Esmaeili, L. Kafi-Ahmadi and S. Khademinia, *J. Mol. Struct.*, 2020, **1216**, 128124–128134.
58 H. Sachdeva, R. Saroj, S. Khaturia and H. L. Singh, *J. Chil. Chem. Soc.*, 2012, **57**, 1012–1016.
59 M. Nasr-Esfahani and T. Abdizadeh, *Phosphorus, Sulfur Relat. Elem.*, 2013, **188**, 596–608.
60 A. Khorshidi, K. Tabatabaeian, H. Azizi, M. Aghaei-Hashjin and E. Abbaspour-Gilandeh, *RSC Adv.*, 2017, **7**, 17732–17740.
61 E. Abbaspour-Gilandeh, A. Yahyazadeh and M. Aghaei-Hashjin, *RSC Adv.*, 2018, **8**, 40243–40251.
62 M. G. Dekamin, F. Mehdipoor and A. Yaghoubi, *New J. Chem.*, 2017, **41**, 6893–6901.
63 K. Godugu, V. D. S. Yadala, M. K. M. Pinjari, T. R. Gundala, L. R. Sanapareddy and C. G. R. Nallagondu, *Beilstein J. Org. Chem.*, 2020, **16**, 1881–1900.
64 R. Tayebee, M. Fattahi Abdizadeh, N. Erfaninia, A. Amiri, M. Baghayeri, R. M. Kakhki, B. Maleki and E. Esmaili, *Appl. Organomet. Chem.*, 2019, **33**, 1–10.
65 K. Niknam, A. Hasaninejad and M. Arman, *Chin. Chem. Lett.*, 2010, **21**, 399–402.
66 L. Shiri, A. Ghorbani-Choghamarani and M. Kazemi, *Monatsh. Chem.*, 2017, **148**, 1131–1139.
67 M. Roozifar, N. Hazeri and H. Faroughi Niya, *J. Heterocycl. Chem.*, 2021, **58**, 1117–1129.
68 G. D. Rao, S. Nagakalyan and G. Prasad, *RSC Adv.*, 2017, **7**, 3611–3616.
69 A. Ghorbani-Choghamarani, Z. Heidarnezhad, B. Tahmasbi and G. Azadi, *J. Iran. Chem. Soc.*, 2018, **15**, 2281–2293.

70 B. Das, M. Srilatha, B. Veeranjaneyulu and B. Shashi Kanth, *Helv. Chim. Acta*, 2011, **94**, 885–891.
71 A. R. Moosavi-Zare, M. A. Zolfigol, M. Zarei, A. Zare and J. Afsar, *Appl. Catal., A*, 2015, **505**, 224–234.
72 X.-H. Yang, P.-H. Zhang, Y.-H. Zhou, C.-G. Liu, X.-Y. Lin and J.-F. Cui, *Arkivoc*, 2011, **10**, 327–337.
73 H. S. Oboudatian, H. Naeimi and M. Moradian, *RSC Adv.*, 2021, **11**, 7271–7279.
74 G. S. Prakash, H. Lau, C. Panja, I. Bychinskaya, S. K. Ganesh, B. Zaro, T. Mathew and G. A. Olah, *Catal. Lett.*, 2014, **144**, 2012–2020.
75 R. Tayebee and M. Ghadamgahi, *Arab. J. Chem.*, 2017, **10**, S757–S764.
76 H. R. Shaterian, A. Hosseinian, M. Ghashang, F. Khorami and N. Karimpoor, *Phosphorus Sulfur Silicon Relat. Elem.*, 2009, **184**, 2333–2338.
77 Q. Zhang, X. Wang, Z. Li, W. Wu, J. Liu, H. Wu, S. Cui and K. Guo, *RSC Adv.*, 2014, **4**, 19710–19715.
78 A. Davoodnia, M. Khashi and N. Tavakoli-Hoseini, *Chin. J. Catal.*, 2013, **34**, 1173–1178.
79 C. S. Reddy and M. Raghu, *Chin. Chem. Lett.*, 2008, **19**, 775–779.
80 D. Aute, A. Kshirsagar, B. Uphade and A. Gadhave, *Res. Chem. Intermed.*, 2020, **46**, 3491–3508.
81 S. Karhale, C. Bhenki, G. Rashinkar and V. Helavi, *New J. Chem.*, 2017, **41**, 5133–5141.
82 T. Tamoradi, M. Ghadermazi and A. Ghorbani-Choghamarani, *Catal. Lett.*, 2018, **148**, 857–872.
83 A. Rajini, M. Nookaraju, I. Reddy and V. Narayanan, *Chem. Pap.*, 2014, **68**, 170–179.